

## MEASURING THE DARK ENERGY WITH QUASAR CLUSTERING

M. O. CALVÃO, J. R. T. DE MELLO NETO, AND I. WAGA

*Universidade Federal do Rio de Janeiro,**Instituto de Física,**CEP 21945-970 Rio de Janeiro, RJ, Brazil**orca@if.uffrj.br, jtmn@if.uffrj.br, ioav@if.uffrj.br**Draft version December 2, 2024*

## ABSTRACT

We show, through Monte Carlo simulations, that the Alcock-Pazynski test, as applied to quasar clustering, is a powerful tool to probe the cosmological density and equation of state parameters,  $\Omega_{m0}$ ,  $\Omega_{x0}$  and  $w$ . By taking into account peculiar velocity corrections to the correlation function we obtain, for the Two-Degree Field QSO Redshift Survey (2QZ), the predicted  $1\sigma$  and  $2\sigma$  confidence contours. It turns out that the test is competitive with future supernova and galaxy number count ones, besides being complementary to them, for fixed curvature. In particular, we find out that it is especially sensitive to the difference  $\Omega_{m0} - \Omega_{\Lambda0}$ , thus being ideal to combine with CMB results.

*Subject headings:* cosmology: theory — cosmological parameters — dark matter

## 1. INTRODUCTION

Recent studies in which type Ia supernovae (SNe Ia) are used as calibrated standard candles suggest that the expansion of the Universe is accelerating, driven by some kind of negative-pressure dark energy (Riess et al. 1999; Perlmutter et al. 1999). Independent evidence for the SNe Ia results is provided by observations of cosmic microwave background (CMB) anisotropies in combination with constraints on the matter density parameter ( $\Omega_{m0}$ ); CMB data favor a nearly flat Universe (de Bernardis et. al. 2000; Balbi et al. 2000; Pryke et al. 2001), while  $\Omega_{m0}$  measurements now point to low values,  $\Omega_{m0} = 0.3 \pm 0.1$  (Bahcall et al. 1999; Turner 2000). The currently favored cosmological model is thus spatially flat, with  $\Omega_{m0} \simeq 1/3$  and a dark energy component with density parameter  $\Omega_{x0} \simeq 2/3$ . The exact nature, however, of this dark energy is not well understood at present. Vacuum energy or a cosmological constant ( $\Lambda$ ) is the simplest explanation, but attractive alternatives like a dynamical scalar field (quintessence) (Ratra & Peebles 1988; Frieman et al. 1995; Caldwell, Dave & Steinhardt 1998; Ferreira & Joyce 1998) have also been explored in the literature. To achieve a better understanding of the nature of the dark energy, an important task nowadays in cosmology is to find new methods that could directly quantify the amount of dark energy present in the Universe as well as determine its equation of state and time dependence. New methods may constrain different regions of the parameter space and are usually subject to different systematic errors, and they are therefore crucial to cross-check (or complement) the SNe results.

The test we focus on here is the one suggested by Alcock & Paczynski (1979) (hereafter AP). This test is based on the fact that transverse (angular separation) and radial (redshift separation) distances have a different dependence on cosmological parameters. Therefore, at high redshift, a spherical object in real space will appear distorted in redshift space. In fact assuming a Euclidean geometry for redshift space, the spherical object will appear elongated along the line of sight. The degree of distortion increases with redshift and is very sensitive to  $\Lambda$  or, more generally, to dark energy. The greatest advantage of the method, as proposed by AP, is that it does not depend on standard candles or standard rods; it is evolution independent.

AP suggested idealized spherical clusters of galaxies to implement their test. However, there are no such idealized objects in nature. Further, the radial and redshift extent of clusters are difficult to measure accurately. During the last years some variants of the original AP test have been proposed (Ryden 1995; Ballinger, Peacock & Heavens 1996; Hui, Stebbins & Burles 1999; McDonald & Miralda-Escudé 1999). Here we are particularly interested in using the QSO correlation function as the “spherical object”.

Because of the isotropy of the Universe, QSOs have, on average, no preferential direction to cluster. However, due to the geometric distortion, they will be more clustered along the line of sight in redshift space. This is the signal to be measured. Popowski et al. (1998) (hereafter PWRO) extended a calculation by Phillipps (1994) of the geometrical distortion of the QSO correlation function. They suggested a simple Monte Carlo experiment to see what constraints should be expected from the 2dF QSO Redshift Survey (2QZ) and the Sloan Digital Sky Survey (SDSS), but they did not estimate the probability density in the parameter space. As a consequence, they were concerned about uncertainties in the determination of  $\Omega_{m0}$  and could not notice that the test is in fact very sensitive to the difference  $\Omega_{m0} - \Omega_{\Lambda0}$ . Further, they did not take into account peculiar velocity corrections, although they discussed their role arguing that it would not overwhelm the geometric signal.

The aim of this Letter is to extend PWRO results in the following aspects: (1) We use Monte Carlo simulations to obtain the expected  $1\sigma$  and  $2\sigma$  confidence level regions in the  $(\Omega_{m0}, \Omega_{\Lambda0})$ -plane for  $\Lambda$ CDM models. With our approach, it is possible to compare the expected constraints on the parameter space from the geometric distortion test when applied to QSO surveys, with those obtained by other methods; (2) We extend the analysis to include a dark energy component with equation of state  $P_x = w \rho_x$ . Here  $w$  is assumed constant, for simplicity. For flat cosmologies, we obtain the  $1\sigma$  and  $2\sigma$  confidence level regions in the  $(\Omega_{m0}, w)$ -plane. Our analysis can be generalized to dynamical scalar field cosmologies as well as to any model with redshift dependent equation of state. Since most quasars have redshift  $z \lesssim 2$  we expect the test to be important in the determination of a possible redshift dependence of the equa-

tion of state; (3) We explicitly take into account linear peculiar velocity corrections. We consider a scale-independent bias parameter, assuming a special form for its redshift dependence; (4) Our calculations are based on the measured 2QZ distribution function and we consider best fit values for the amplitude and exponent of the correlation function as obtained by Croom et al. (2001). In this Letter, we only consider the 2QZ survey although the results can easily be generalized to SDSS. Since the quasar clustering is more sensitive to the QSO number density than to their total number (cf. PWRO), we expect tighter constraints on the parameter space from the 2QZ survey.

## 2. BASICS

We assume that the geometry is described by the standard Robertson-Walker metric. The source is characterized by only two appreciable components: (i) a collisionless non-relativistic matter (including baryons and CDM) with energy density  $\rho_m$ , and (ii) an exotic dark energy with energy density  $\rho_x$  and typically negative pressure  $P_x$ . We will furthermore assume that both kinds of matter do not interact and that the dark energy has the usual linear barotropic equation of state  $P_x = w\rho_x$ , with  $w$  constant. The dynamics of the model is governed by general relativity, which furnishes

$$\Omega_m + \Omega_x + \Omega_k = 1, \quad (1)$$

$$q = \frac{1}{2} [\Omega_m + (1+3w)\Omega_x], \quad (2)$$

where the above quantities have their usual meaning. Notice that these quantities are defined for any epoch, their present values being denoted by a 0 subscript.

By a straightforward calculation for null geodesics, we can obtain a generalized Mattig relation, providing the radial coordinate  $R$  as a function of  $z$ :

$$a_0 R = f(z) := \begin{cases} \sinh \{ \sqrt{\Omega_{k0}} I(z) \} / (H_0 \sqrt{\Omega_{k0}}), & \Omega_{k0} > 0, \\ I(z), & \Omega_{k0} = 0, \\ \sin \{ \sqrt{-\Omega_{k0}} I(z) \} / (H_0 \sqrt{-\Omega_{k0}}), & \Omega_{k0} < 0, \end{cases} \quad (3)$$

where  $a_0$  is the present scale factor,

$$I(z) := \int_{z'=0}^z [H_0 / H(z')] dz', \quad (4)$$

and the Hubble parameter is given by

$$H(z) = H_0 \sqrt{\Omega_{m0}(1+z)^3 + \Omega_{x0}(1+z)^{3(1+w)} + \Omega_{k0}(1+z)^2}. \quad (5)$$

Given two close point sources (e.g., quasars), with coordinates  $(z, \theta, \phi)$  and  $(z+dz, \theta+d\theta, \phi+d\phi)$ , directly read off a catalogue, the real-space infinitesimal comoving distance between them can be decomposed, in the distant observer approximation we will adopt here, into contributions parallel and perpendicular to the line of sight,

$$r_\perp := f(z) d\alpha, \quad r_{||} := \frac{1}{H(z)} dz, \quad (6)$$

such that  $r^2 = r_{||}^2 + r_\perp^2$ . Here,  $d\alpha$  is the small angle between the lines of sight.

The gist of AP test relies then on the clear fact that, if we observe an intrinsically spherical system ( $r_{||} = r_\perp$ ), it will appear distorted, in redshift space, according to the generic formula

$$\frac{r_\perp}{r_{||}} = j(z) \frac{s_\perp}{s_{||}}, \quad (7)$$

where the anisotropy or distortion function  $j(z)$  is defined by

$$j(z) := \frac{f(z)H(z)}{z}. \quad (8)$$

Here we have assumed a Euclidean geometry for redshift space, that is,  $s_{||} := dz$ ,  $s_\perp := zd\alpha$ , and  $s^2 = s_{||}^2 + s_\perp^2$ . We also introduce the director cosine  $\mu := s_{||}/s$ . A simple analysis of the distortion function for several typical models reveals that: (i) a spherical system is squashed perpendicular to the line of sight [ $j(z) > 1$ ], (ii) the distorting effect is the more prominent the higher the redshift, (iii) the test is rather discriminatory between  $\Omega_{x0} = 0$  open models and  $\Omega_{m0} + \Omega_{x0} = 1$  flat models. In fact, as we will see in the next sections, for  $w = -1$ , the test is very sensitive to the difference  $\Omega_{m0} - \Omega_{\Lambda0}$ .

Generically, the following relation between the real-space distance  $r$  and the redshift-space “distance”  $s$  holds:

$$\frac{r}{s} = \frac{\sqrt{\mu^2 + j^2(z)(1-\mu^2)}}{H(z)}. \quad (9)$$

## 3. QUASAR CLUSTERING AND MONTE CARLO SIMULATIONS

Observations (Croom et al. 2001) suggest that the correlation function for quasars, in real space, is reasonably well fitted by a power law,

$$\xi(r) = \left( \frac{r}{r_0} \right)^{-\gamma}, \quad (10)$$

with  $r_0 \simeq 5 h^{-1}$  Mpc and  $\gamma \simeq 2$ . We then have, in redshift space, an anisotropic correlation function, given by

$$\xi(s, \mu) = \left( \frac{s}{s_0(z)} \right)^{-\gamma} [\mu^2 + j^2(z)(1-\mu^2)]^{-\gamma/2}, \quad (11)$$

where

$$s_0(z) := r_0 H(z). \quad (12)$$

Peculiar velocities also induce distortions in the correlation function which can be confused with those arising from the cosmological geometric effect. It is important to take them into account when comparing theory with observations. As argued by PWRO, non-linear corrections are likely to be small and we neglect them in our analysis. The relevant effect to be considered is due to large-scale coherent flows (Kaiser 1987).

The linear theory corrected correlation function is given by (Hamilton 1992; Matsubara & Suto 1996),

$$\xi_{corr}(s, \mu) = \left[ \left( 1 + \frac{2\beta}{3} + \frac{\beta^2}{5} \right) P_0(\bar{\mu}) + \left( \frac{4\beta}{3} + \frac{4\beta^2}{7} \right) \frac{\gamma}{\gamma-3} P_2(\bar{\mu}) + \frac{8\beta^2}{35} \frac{\gamma(\gamma+2)}{(5-\gamma)(3-\gamma)} P_4(\bar{\mu}) \right] \xi(r), \quad (13)$$

where the  $P_i(\bar{\mu})$  are Legendre polynomials, and  $\bar{\mu} := r_{||}/r$ . As usual, in the above expression,  $\beta(z) := f(z)/b(z)$ ,  $f(z) = -d \ln \Delta_+ / d \ln(1+z)$  is the linear growth rate, and we adopt the following dependence for the bias parameter  $b(z)$ :

$$b(z) = 1 + \left( \frac{\Delta_+(z=0)}{\Delta_+(z)} \right)^m (b_0 - 1). \quad (14)$$

If  $m = 1$ , we have the linear theory redshift dependence for the bias (Fry 1996). The case  $m = 0$  corresponds to a constant bias, and we also use  $m \simeq 1.7$  in our computations, which seems to be more in accordance with an observed non-evolving clustering (Croom et al. 2001). For models where the dark energy is a

cosmological constant ( $w = -1$ ), we use the Heath solution for the growing mode (Heath 1977),

$$\Delta_+(z) = \frac{5}{2} \Omega_{m0} H(z) \int_z^\infty \frac{1+x}{H(x)^3} dx \quad (w = -1), \quad (15)$$

and the following approximation for the growth rate (Lahav et al. 1991),

$$f(z) \simeq \Omega_m^{4/7}(z) + \frac{\Omega_\Lambda(z)}{70} \left( 1 + \frac{\Omega_m(z)}{2} \right) \quad (w = -1). \quad (16)$$

For flat models, Silveira & Waga (1994) obtained an exact solution for the growing mode,

$$\begin{aligned} \Delta_+(z) &= \left( \frac{1}{1+z} \right) \\ &\times {}_2F_1 \left[ -\frac{1}{3w}, \frac{w-1}{2}, 1 - \frac{5}{6w}; \frac{1-\Omega_{m0}}{\Omega_{m0}} (1+z)^{3w} \right] (\Omega_k = 0), \end{aligned} \quad (17)$$

where  ${}_2F_1[a, b, c; x]$  is the hypergeometric function. The growth rate can also be expressed in terms of hypergeometric functions, but for the sake of simplicity we shall not exhibit it here.

Following PWRO, we obtain, for the number of pairs expected in an infinitely small bin within  $(z, s, \mu)$  and  $(z+dz, s+ds, \mu+d\mu)$ ,

$$dN_{pairs} = -\frac{2\pi}{A} \left( \frac{180 N_Q F(z)}{\pi z} \right)^2 [1 + \xi_{corr}(s, \mu)] s^2 dz ds d\mu. \quad (18)$$

Here  $A$  is the area (in square degrees) of the survey,  $N_Q$  is the total number of sources (quasars) in the survey, and  $F(z)$  is the normalized distribution function.

Croom et al. (2001), assuming an Einstein-de Sitter Universe ( $\Omega_m = 1, \Omega_\Lambda = 0$ ), showed that the quasar clustering amplitude  $r_0$  appears to vary very little over the entire redshift range of the 2QZ survey. They found  $r_0 \simeq 4 h^{-1}$  Mpc as their best fit, which remains nearly constant in comoving coordinate. Therefore, we have

$$s_0|_{EdS}(z) := H(z)|_{EdS} r_0 = \frac{4}{3000} (1+z)^{3/2}. \quad (19)$$

Following again PWRO, we use the fact that the total number of correlated pairs,  $N_{pairs}$ , in the survey is model independent to scale (19) to other cosmologies. It is straightforward to show that  $N_{pairs} \propto s_0^3(z) / j^2(z)$ , and we use

$$s_0(z, \Omega_{m0}, \Omega_{\Lambda0}, w) = \frac{4}{3000} (1+z)^{3/2} \left[ \frac{j(z, \Omega_{m0}, \Omega_{\Lambda0}, w)}{j|_{EdS}(z)} \right]^{2/3}, \quad (20)$$

as a fiducial redshift-space correlation length for our simulations.

A particular model for the correlation function may depend on several parameters ( $\Omega_{m0}, \Omega_{\Lambda0}, w, r_0, \gamma, b_0, m, \dots$ ). Given the model, it predicts a number of pairs  $A_i$  in each bin of a  $(z, s, \mu)$  space. In a real (or simulated) situation the data consists of  $N_i$  pairs in  $i$  bins. PWRO showed that for typical surveys, such as SDSS and 2QZ, we are bound to be in the “sparse regime” or “Poisson limit”. In this case we may treat bins in  $(z, s, \mu)$  space as independent and the probability of detecting  $N_i$  pairs in bin  $i$ , when  $A_i$  are expected, is

$$P(N_i|A_i) = \frac{e^{-A_i} A_i^{N_i}}{N_i!} \quad (21)$$

Since the bins are independent, the likelihood  $\mathcal{L}$  of obtaining the data given the model is simply the product,  $\mathcal{L} = \prod_i P(N_i|A_i)$ . For a typical 2QZ simulation (we also ran SDSS simulations), we assumed: (i) the completed survey will comprise  $N_Q = 26000$  quasars in a total area  $A = 750$  square degrees; (ii) the Einstein-de Sitter fiducial correlation function has  $r_0 = 4 h^{-1}$  Mpc and  $\gamma = 1.6$ ; (iii) the bias model is characterized by  $b_0 = 1.5$  and  $m = 1$ . The linear binning we chose covered the ranges:  $0.4 < z < 2.6$ ,  $0.2 < s/s_0(z) < 7$ , and  $0 < \mu < 1$ , with 16 bins in  $z$ , 34 in  $s/s_0(z)$ , and 5 in  $\mu$ , making up a total of 2720 bins. The maximization of the likelihood was carried out with MINUIT (James 1994) and cross-checked with MATHEMATICA. The probability density function was built via a Gaussian kernel density estimate, from typically 1000 runs for each “true” model.

#### 4. RESULTS

We first analyze the case of a conventional cosmological constant ( $w = -1$ ) in a universe with arbitrary spatial curvature. In Figure 1, we show the predicted AP likelihood contours in the  $(\Omega_{m0}, \Omega_{\Lambda0})$ -plane for the 2QZ survey (solid lines). The points in the figure represent maximum likelihood values for  $\Omega_{m0}$  and  $\Omega_{\Lambda0}$  obtained with Monte Carlo simulations as explained in the previous section. The assumed “true” values for Figure 1 are, from top to bottom,  $(\Omega_{m0} = 0.3, \Omega_{\Lambda0} = 0)$ ,  $(\Omega_{m0} = 0.28, \Omega_{\Lambda0} = 0.72)$  and  $(\Omega_{m0} = 0.73, \Omega_{\Lambda0} = 1.32)$ . In the top panel the displayed curve corresponds to the predicted  $2\sigma$  likelihood contour. In the middle panel the predicted  $1\sigma$  contour (dashed line) for one year of SNAP data (Goliath et al. 2001) is displayed, together with the predicted  $1\sigma$  AP contour. For the SNAP contour, it is also assumed that the intercept  $\mathcal{M}$  is exactly known. In the bottom panel,  $\Omega_{m0}$  and  $\Omega_{\Lambda0}$  were chosen to have some ground of comparison with current SNe Ia observations. These values are the best fit  $\Omega_{m0}$  and  $\Omega_{\Lambda0}$  (fit C) obtained by Perlmutter et al. (1999) and, in the same panel, we also plot their  $1\sigma$  and  $2\sigma$  contours (dashed lines) together with the  $2\sigma$  predicted AP contour. As expected, in all cases, the test recovers nicely the “true” values. We stress out that the test is very sensitive to the difference  $\Omega_{m0} - \Omega_{\Lambda0}$ . From the middle panel we note that the sensitivity to this difference is comparable to that expected from SNAP, of the order  $\pm 0.01$ . The sensitivity increases for higher values of  $\Omega_{\Lambda0}$ . Comparatively, however, the test has a larger uncertainty in the determination of  $\Omega_{m0} + \Omega_{\Lambda0}$ , of the order  $\pm 0.17$ . Again the uncertainty decreases as we increase  $\Omega_{\Lambda0}$ . The degeneracy in  $\Omega_{m0} + \Omega_{\Lambda0}$  may be broken if we combine the estimated results for the geometric test with, for instance, those from CMB anisotropy measurements, whose contour lines are orthogonal to those exhibited in the panels (Hu et al. 1999).

In obtaining Figure 1, we considered linear peculiar velocity corrections in the generation of the expected “true”  $A_i$  values and also in the computations to find the maximum likelihood in all the runs. In order to estimate the consequences of neglecting these corrections, in Figure 2, we included them in the calculation of the  $A_i$  values but neglected them in the computation of the maximum likelihood; in this figure, we assume  $\Omega_{m0} = 0.3$  and  $\Omega_{\Lambda0} = 0$  as “true” values. Notice that the point with the “true”  $\Omega_{m0}$  and  $\Omega_{\Lambda0}$  values is outside the  $2\sigma$  contour. It is clear, therefore, the necessity of taking those effects in consideration when analyzing real data.

Another important point is to assess how sensitive the test is to the biasing evolution. To illustrate that it is in fact more sensitive to the mean amplitude of the bias rather than to its exact

redshift dependence, we plot, in Figure 3, the  $2\sigma$  contour line, assuming as “true” values  $\Omega_{m0} = 0.3$  and  $\Omega_{\Lambda0} = 0.7$ . For this figure, the “true”  $A_i$  values were generated assuming  $b_0 = 1.45$  and  $m = 1.68$ . However, for the simulations, we considered a constant bias ( $m = 0$ ), such that  $b_{0,sim} := \int_{z=z_{min}}^{z_{max}} F(z)b_{true}(z)dz = 2.46$ . We remark that the contour is slightly enlarged, mainly in the direction of the “ellipsis” major axis. However, the uncertainty in  $\Omega_{m0} - \Omega_{\Lambda0}$  is practically unaltered, confirming the strength of the test (Yamamoto & Nishioka 2001).

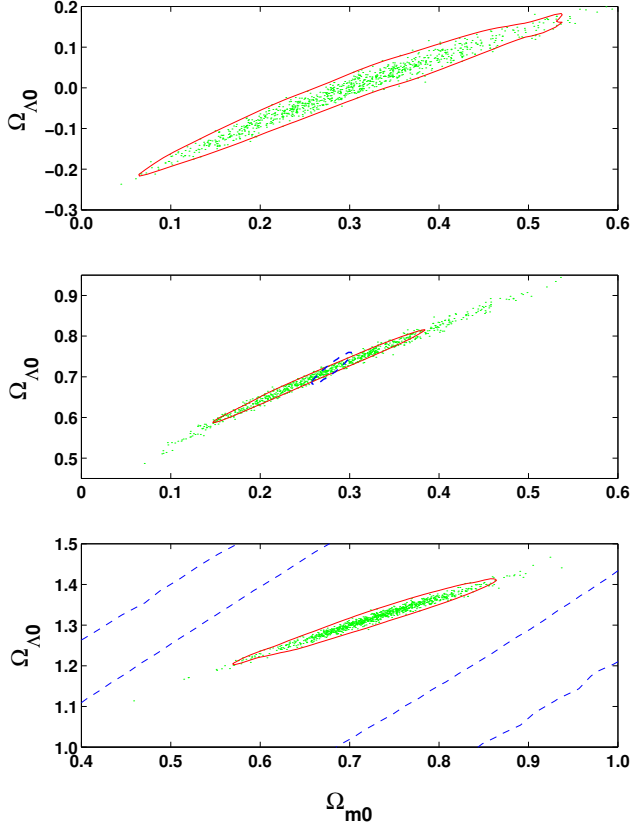


FIG. 1.— Simulated models at fixed  $w = -1$  and corresponding predicted AP confidence contours (solid lines); both the “true” model and the simulated ones take into account the linear effect from peculiar velocities. In the top panel we show the predicted  $2\sigma$  likelihood contour assuming a “true” model ( $\Omega_{m0} = 0.3, \Omega_{\Lambda0} = 0$ ). In the middle panel the predicted  $1\sigma$  contour (dashed line) for one year of SNAP data (Goliath et al. 2001) is displayed, together with the predicted  $1\sigma$  AP contour. For both tests we consider  $\Omega_{m0} = 0.28, \Omega_{\Lambda0} = 0.72$  and for the SNAP result it is assumed that the intercept  $\mathcal{M}$  is exactly known. The bottom panel is from a “true” model ( $\Omega_{m0} = 0.73, \Omega_{\Lambda0} = 1.32$ ), and besides the  $2\sigma$  AP contour, it also displays the corresponding  $1\sigma$  and  $2\sigma$  observed SCP confidence contours [dashed lines; Perlmutter et al. (1999)].

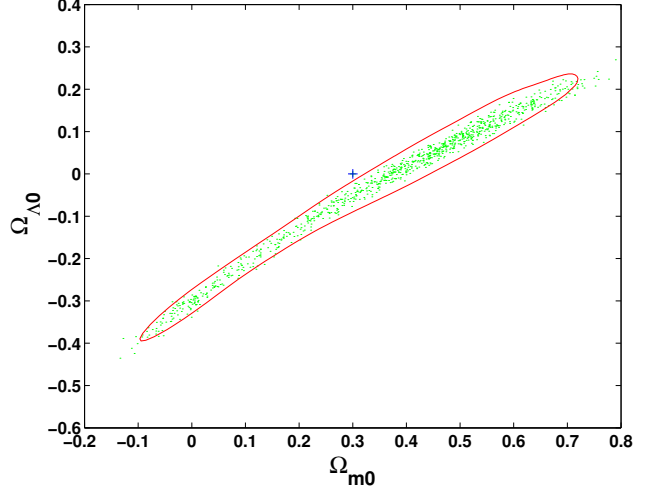


FIG. 2.— Simulated models at fixed  $w = -1$  and corresponding  $2\sigma$  predicted AP confidence contour. The “true” model ( $\Omega_{m0} = 0.3, \Omega_{\Lambda0} = 0$ ) takes into account the peculiar velocity corrections, but the simulated ones do not. Notice that the “true” model (the cross in the figure) does not fall into the  $2\sigma$  confidence region.

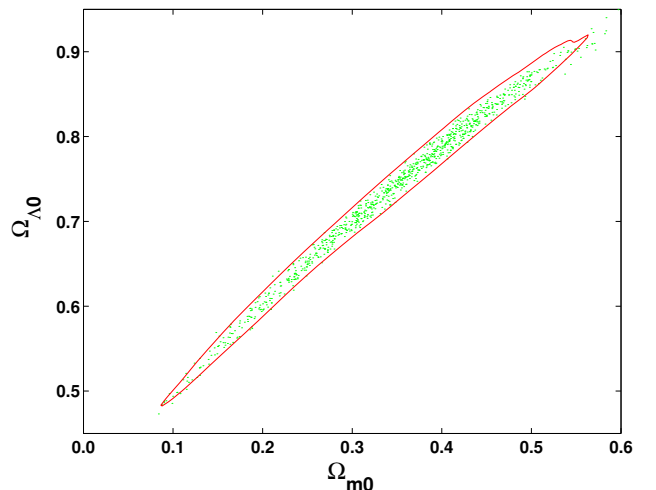


FIG. 3.— Simulated models at fixed  $w = -1$  and corresponding  $2\sigma$  predicted AP confidence contour; both the “true” model ( $\Omega_{m0} = 0.3, \Omega_{\Lambda0} = 0.7$ ) and the simulated ones take into account the linear effect from peculiar motions. The “true” model uses a redshift-dependent bias function with  $b_0 = 1.45$  and  $m = 1.68$ , whereas the simulated ones use a constant bias equal to 2.46.

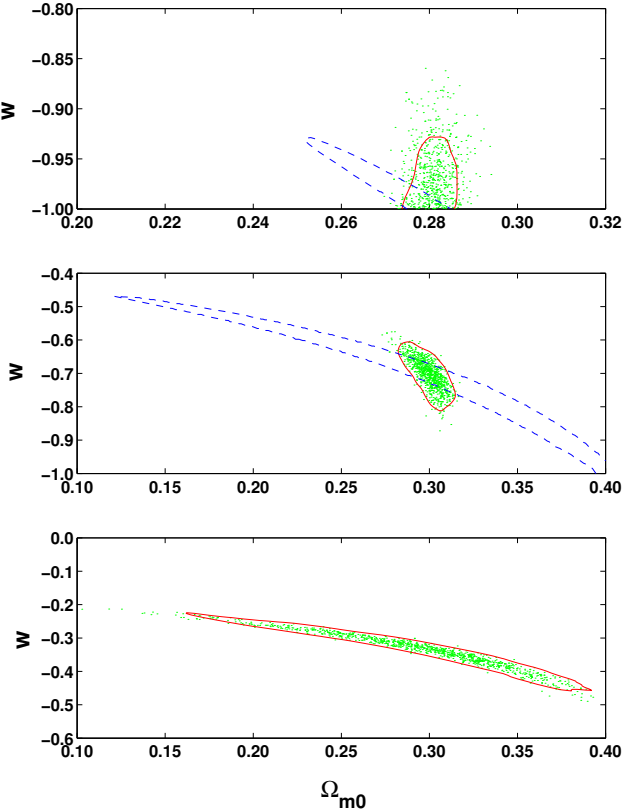


FIG. 4.— Simulated models at fixed  $\Omega_{k0} = 0$  and corresponding predicted AP confidence contours (solid lines); both the “true” model and the simulated ones take into account the linear effect from peculiar velocities. The top panel is from a “true” model ( $\Omega_{m0} = 0.28, \Omega_{x0} = 0.72, w = -1$ ), and displays the predicted confidence contours for the AP test and the SNAP mission [dashed line; Goliath et al. (2001)], both at  $1\sigma$  level. The middle panel is from a “true” model ( $\Omega_{m0} = 0.3, \Omega_{x0} = 0.7, w = -0.7$ ), and displays the predicted confidence contours for the AP test and the DEEP survey [dashed line; Newman & Davis (2000)], both at the  $95\%$  level. The bottom panel is from a “true” model ( $\Omega_{m0} = 0.3, \Omega_{x0} = 0.7, w = -1/3$ ) and just shows the  $2\sigma$  predicted contour for the AP test.

Now we analyze the case of flat models ( $\Omega_{k0} = 0$ ), with arbitrary  $w$ . In Figure 4, we show the predicted AP likelihood contours in the  $(\Omega_{m0}, w)$ -plane for the 2QZ survey (solid lines). The “true” values for Figure 4 are, from top to bottom,  $(\Omega_{m0} = 0.28, w = -1)$ ,  $(\Omega_{m0} = 0.3, w = -0.7)$ , and  $(\Omega_{m0} = 0.3, w = -1/3)$ . In the top panel, we show, besides the AP contour, the predicted contour for one year of SNAP data [dashed line; Goliath et al.

(2001)], both at  $1\sigma$  level. For the SNAP contour, the intercept  $\mathcal{M}$  is assumed to be exactly known. Notice that the contours are somewhat complementary and are similar in strength. In the middle panel, we compare the predicted  $95\%$  confidence contour of the AP test with the same confidence level contour for the number count test as expected from the DEEP redshift survey [dashed line; Newman & Davis (2000)]. Again the contours are complementary, but the uncertainties on  $\Omega_{m0}$  and  $w$  for the AP test are quite smaller. Finally, in the bottom panel, we just show the estimated  $2\sigma$  AP likelihood contour.

## 5. CONCLUSION

We have shown that the Alcock-Pazynski test applied to the 2dF quasar survey (2QZ) is a potent tool for measuring cosmological parameters. We stress out that the test is especially sensitive to  $\Omega_{m0} - \Omega_{\Lambda 0}$ . We have established that the expected confidence contours are in general complementary to those obtained by other methods and we again emphasize the importance of combining them to constrain even more the parameter space. We have also revealed that, for fixed  $\Omega_{m0} + \Omega_{\Lambda 0}$ , the estimated constraints are similar in strength to those from SNAP with the advantage that the 2QZ survey will soon be completed.

Of course our analysis can be improved in several aspects. For instance, we have assumed that  $\gamma$  and  $r_0$  do not depend on redshift. In fact, observations (Croom et al. 2001) seem to support these assumptions, but further investigations are necessary. Also, in our simulations, we assumed fixed values for some quantities, like  $\gamma$  and  $r_0$ , without taking into account possible uncertainties in their determination. This will be incorporated in our future simulations. At present, the quasar clustering bias is not completely well understood. Theoretical as well as observational progress in its determination will certainly improve the real capacity of the test. However, confirming previous investigations (Yamamoto & Nishioka 2001), we have found that the test is, in fact, more sensitive to the mean amplitude of the bias rather than to its exact redshift dependence. Further investigations on the role of bias and some other aspects that could not be discussed here at length will be published elsewhere.

We would like to thank J. Silk for calling attention to the potential of the AP test and T. Kodama for some helpful suggestions regarding numerical issues. We also thank the Brazilian research agencies CNPq, FAPERJ and FUJB.

## REFERENCES

Alcock, C. & Paczyński, B. 1979, *Nature*, **281**, 358 [AP].  
 Bahcall, N. A., Ostriker, J. P., Perlmutter, S. & Steinhardt, P. J. 1999, *Science*, **284**, 1481.  
 Balbi, A. et al. 2000, *ApJ*, **545**, L1.  
 Ballinger, W. E., Peacock, J. A. & Heavens, A. F. 1996, *MNRAS*, **282**, 877.  
 Caldwell, R. R., Dave, R. & Steinhardt, P. J. 1998, *Phys. Rev. Lett.*, **80**, 1582.  
 Croom, S. M. et al. 2001, *MNRAS*, in press (astro-ph/0012375).  
 de Bernardis, P. et al. 2000, *Nature*, **404**, 955.  
 Ferreira, P. & Joyce, M. 1998, *Phys. Rev. D*, **58**, 023503.  
 Frieman, J. A., Hill, C. T., Stebbins, A. & Waga, I. 1995 *Phys. Rev. Lett.*, **75**, 2077.  
 Fry, J. N. 1996, *ApJ*, **461**, L65.  
 Goliath, M., Amanullah, R., Astier, P., Goobar, A. & Pain, R. 2001, *A&A*, submitted (astro-ph/0104009).  
 Hamilton, A. J. S. 1992 *ApJ*, **385**, L5.  
 Heath, D. J. 1977, *MNRAS*, **179**, 351.  
 Hu, W., Eisenstein, D. J., Tegmark, M. & White, M. 1999, *Phys. Rev. D*, **59**, 023512.  
 Hui, L., Stebbins, A. & Burles, S. 1999, *ApJ*, **511**, L5.  
 James, F. 1994, MINUIT Reference Manual Version 94.1, CERN Program Library Long Writeup D506, CERN.  
 Kaiser, N. 1987, *MNRAS*, **227**, 1.  
 Lahav, O., Lijle, P. B., Primack, J. R. & Rees, M. J. 1991, *MNRAS*, **251**, 136.  
 Matsubara, T. & Suto, Y. 1996, *ApJ*, **470**, L1.  
 McDonald, P. & Miralda-Escudé, J. 1999, *ApJ*, **518**, 24.  
 Newman, J. F. & Davis, M. 2000, *ApJ*, **534**, L11.  
 Perlmutter, S. et al. 1999, *ApJ*, **517**, 565.  
 Phillips, S. 1994, *MNRAS*, **269**, 1077.  
 Popowski, P. A., Weinberg, D. H., Ryden, B. S. & Osmer, P. S. 1998 *ApJ*, **498**, 11 [PWRO].  
 Pryke, C. et al. 2001, *ApJ*, submitted (astro-ph/0104490).  
 Ratra, B. & Peebles, P. J. E. 1988, *Phys. Rev. D*, **37**, 3406.  
 Riess, A. G. et al. 1999, *AJ*, **116**, 1009.  
 Ryden, B. S. 1995, *ApJ*, **452**, 25.  
 Silveira, V. & Waga, I. 1994, *Phys. Rev. D*, **50**, 4890.  
 Turner, M. S. 2000, *Physica Scripta*, **T85**, 210.  
 Yamamoto, K. & Nishioka, H. 2001, *ApJ*, **549**, L15.